nature biotechnology

Evolutionary optimization of fluorescent proteins for intracellular FRET

Annalee W Nguyen[1] & Patrick S Daugherty[1]

Fluorescent proteins that exhibit Förster resonance energy transfer (FRET) have made a strong impact as they enable measurement of molecular-scale distances through changes in fluorescence[1]. FRET-based approaches have enabled otherwise intractable measurements of molecular concentrations[2], binding interactions[3] and catalytic activity[4], but are limited by the dynamic range and sensitivity of the donor-acceptor pair. To address this problem, we applied a quantitative evolutionary strategy using fluorescence-activated cell sorting to optimize a cyan-yellow fluorescent protein pair for FRET. The resulting pair, CyPet-YPet, exhibited a 20-fold ratiometric FRET signal change, as compared to threefold for the parental pair. The optimized FRET pair enabled high-throughput flow cytometric screening of cells undergoing caspase-3–dependent apoptosis. The CyPet-YPet energy transfer pair provides substantially improved sensitivity and dynamic range for a broad range of molecular imaging and screening applications.

The small dynamic range of fluorescent protein FRET yields poor sensitivity for many applications[5,6]. Though synthetic FRET pairs can exhibit a dynamic range of 100-fold or more[7], that of typical fluorescent protein pairs is just four- to fivefold[8]. In addition, measurement of FRET is hindered by overlap between the donor and acceptor emission spectra and excitation of the acceptor at donor excitation wavelengths[1]. Collectively, these problems have slowed the development of intracellular imaging and high-throughput screening tools that use FRET. Fluorescent proteins better suited for FRET would be of great utility[9], enabling new high-throughput screening applications using flow cytometry. Consequently, we designed an evolutionary strategy to enable coupled evolution of the FRET dynamic range of a cyan-yellow fluorescent protein (CFP-YFP) pair. We hypothesized that screening of appropriately diverse libraries directly for FRET using sensitive fluorescence-activated cell sorting (FACS) instrumentation would enable discrimination and enrichment of even subtle improvements, allowing gradual evolutionary optimization of FRET signals. Highly effective FRET pairs were evolved using four FRET evolutionary cycles consisting of mutagenesis and synthetic DNA shuffling, followed by sequential FACS and fluorimetric screening (**Fig. 1a**).

To enable efficient library construction and screening directly for improved FRET, we developed a bacterial expression system for regulated expression of tandem fluorescent proteins exhibiting FRET. Genes encoding enhanced (E)CFP and a YFP variant (S65G, S72A, K79R, T203Y) possessing a high extinction coefficient[1] were joined by a sequence encoding a 20-amino acid linker incorporating the caspase-3 cleavage site (DEVD). Expression conditions were optimized to enable detection of FRET between CFP and YFP in *Escherichia coli*. Use of a low copy plasmid and induction at reduced temperatures (25 °C) were found to be important to minimize intracellular aggregation and increase intracellular FRET signals. Even after optimization of expression conditions, the parental CFP-YFP possessed a maximum FRET-ratio change (RRC) of just threefold (**Fig. 1b**). Here, the RRC is the ratio of acceptor fluorescence to donor fluorescence during FRET divided by the ratio in the absence of FRET.

Mutagenesis and screening of both CFP and YFP were performed to evolve pairs exhibiting improved RRC and brightness in whole cells (**Fig. 1a**). Given the difficulty of applying rational design to improve FRET, we used random mutagenesis to identify amino acid residues influencing FRET, which were subsequently targeted for partial or complete saturation mutagenesis through synthetic shuffling. In the initial round, YFP was randomly mutated using error-prone PCR and screened for improvements in brightness and RRC, resulting in YFP2 (**Fig. 1a–c**). The mutations occurring in several improved YFP variants from the first round of screening were synthetically shuffled to create a second smaller *yfp* pool, which was in turn fused to a randomly mutated *cfp* gene pool, and this library was similarly screened for RRC improvements. Interestingly, improvements in the RRC exhibited by the CFP2-YFP3 pair (**Fig. 1b,c**) were the result of substitutions in YFP rather than CFP (data not shown). YFP3 possessed six mutations (**Table 1**) that resulted in an RRC almost fivefold greater than that of the parental pair (**Fig. 1b**). YFP3 also conferred a roughly threefold improvement in FRET relative to the fast-maturing Venus[10] YFP (**Fig. 1b**). In an attempt to further enhance YFP3 brightness, the Venus mutations were combined with those of YFP3 to yield YFP for energy transfer (YPet). Despite similar photophysical properties (**Table 2**), CFP2-YPet and CFP2-YFP3 exhibited an RRC nearly threefold greater than that of CFP-Venus (**Fig. 1b**). Additionally, the CFP2-YPet pair possessed enhanced relative brightness in the RET-on state relative to that of CFP-Venus (**Fig. 1c**). Both YFP3 and YPet exhibited reduced pH sensitivity, possessing pK_a values of 5.79 and 5.63, respectively, when compared with that of Venus (pK_a = 6.29) (**Table 2**). Though YFP3 exhibited slower folding relative

[1]Department of Chemical Engineering, University of California, Santa Barbara, California 93106-5080, USA. Correspondence should be addressed to P.S.D. (psd@engineering.ucsb.edu).

Published online 6 February 2005; doi:10.1038/nbt1066

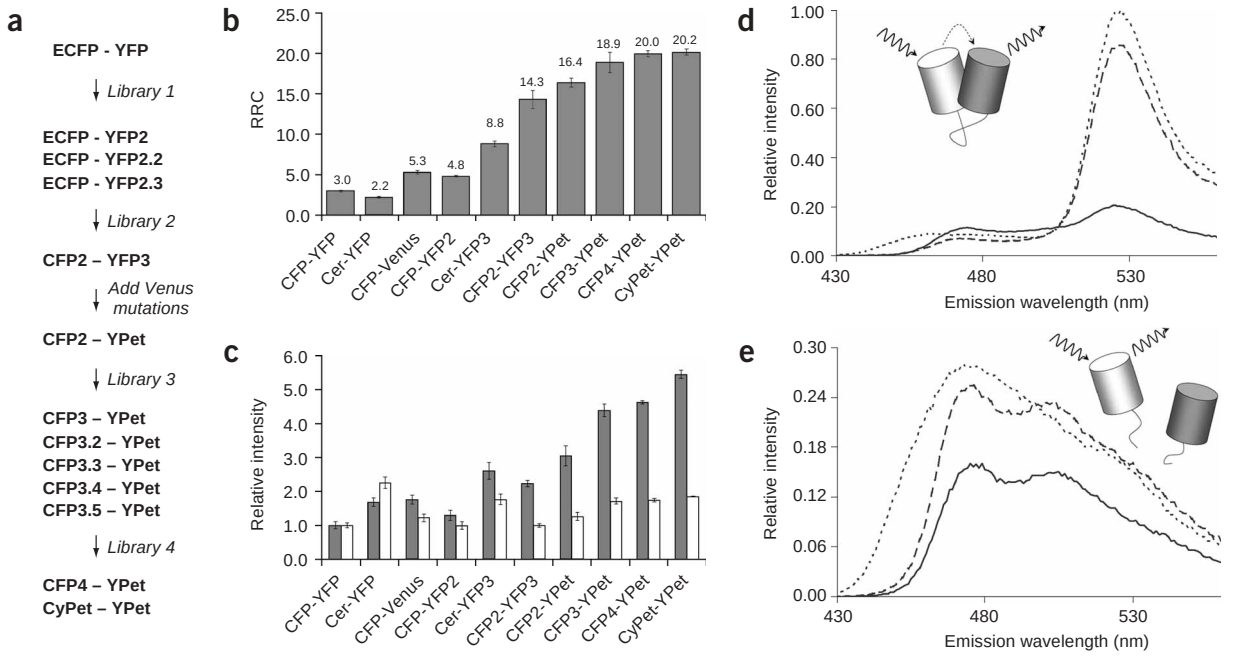

Figure 1 Evolution of FRET pair dynamic range (RRC) and brightness. (**a**) Evolutionary process applied to optimize FRET between CFP and YFP. (**b**) The ratiometric FRET signal was measured before and after cleavage with trypsin *in vitro*. (**c**) The maximum fluorescence intensity was measured in the FRET-on (gray bars) and FRET-off (white bars) states and compared. Values are the average of triplicate measurements and the error is the standard deviation of those measurements (see Methods). (**d**,**e**) Normalized emission spectra of wild-type (solid line) and optimized CFP-YFP FRET pairs CyPet-YPet (dotted line) and CFP4-YPet (dashed line) (**d**) before and (**e**) after trypsin cleavage *in vitro*.

to Venus, combining YFP3 and Venus mutations resulted in intermediate folding kinetics ($k_{fold} = 3.6 \times 10^{-3}$ s^{-1}) (**Table 2**).

The bright CFP variant, Cerulean, possesses an improved quantum yield and extinction coefficient[5], suggesting that it might enhance FRET. Cerulean-YFP (Cer-YFP) was brighter in both FRET-on and FRET-off states (**Fig. 1c**), but possessed an RRC even lower than the parental CFP-YFP pair (**Fig. 1b**). Given this, mutagenesis and screening was applied to further improve the CFP2 donor. A library of randomly mutated CFP variants was constructed, and variants exhibiting improved brightness in whole cells were enriched using FACS. This enriched pool of CFP variants was then paired with YPet and screened for increased RRC, resulting in the CFP3 mutant. The amino acid positions identified in the best CFP variants from this round were used to construct a synthetically shuffled library that was subsequently screened for brightness and RRC. The shuffled CFP library was screened by multistep enrichment using three rounds of FACS for increased whole-cell brightness (**Supplementary Fig. 1** online). Cell populations resulting from successive rounds of FACS

Table 1 YFP and CFP substitutions occurring during multiple rounds of directed evolution

	YFP amino acid positions										
Clone	46	47	64	79	153	163	175	208	224	231	234
YFP	F	I	F	R	M	V	S	S	V	H	D
YFP2									I		
YFP3	L	L						F	L	E	N
Venus	L		L	K	T	A	G				
YPet	L	L	L	K	T	A	G	F	L	E	N

	CFP amino acid positions							
	9	11	19	87	139	167	172	194
ECFP	T	V	D	A	H	I	E	L
CFP2				V				
CFP3	S			V	R	L	G	
CFP4			Q	V			V	N
CyPet	G	I	E	V		A	T	I

Blank spaces indicate wild-type residues.

Table 2 Photophysical properties of CFP and YFP mutants

Clone	k_{fold} ($\times 10^3$) s^{-1}	k_{ox} ($\times 10^3$) s^{-1}	pK_a	ε ($\times 10^{-3}$) $M^{-1}cm^{-1}$	QY	Rel FL
ECFP	3.2 ± 0.7	1.2 ± 0.3	5.51 ± 0.01	27 ± 1	0.58 ± 0.03	1.00 ± 0.01
CFP4	5.0 ± 0.6	2.2 ± 0.2	4.85 ± 0.03	35 ± 3	0.46 ± 0.01	1.59 ± 0.04
CyPet	5.1 ± 0.9	1.8 ± 0.4	5.02 ± 0.02	35 ± 2	0.51 ± 0.01	1.18 ± 0.09
Venus	6.6 ± 0.1	3.2 ± 0.4	6.29 ± 0.01	107 ± 7	0.76 ± 0.02	1.00 ± 0.09
YFP3	1.2 ± 0.1	0.6 ± 0.2	5.79 ± 0.04	99 ± 4	0.76 ± 0.02	0.76 ± 0.03
YPet	3.6 ± 0.2	1.6 ± 0.3	5.63 ± 0.03	104 ± 9	0.77 ± 0.02	0.49 ± 0.04

Each value indicates the average of duplicate measurements and the error is the standard deviation of those measurements. QY: quantum yield; Rel FL: relative whole-cell fluorescence.

exhibited subtle, cumulative increases in whole-cell cyan fluorescence intensity. Subsequently, the improved pool of CFP donors was genetically fused with YPet and screened for high FRET-on signals via FACS (**Supplementary Fig. 1** online). The last round of screening resulted in two variants, CFP4 and CyPet, with similar FRET properties, but differing spectral shapes (**Fig. 1d,e**). Aside from this difference, the photophysical properties of the CFP variants were similar to those of the parental CFP. However, the pK_a and folding rates of CyPet were improved relative to ECFP (**Table 2**). The fluorescence decay kinetics of ECFP, CFP4 and CyPet were best fit by a biexponential function either in the presence or absence of a YFP acceptor (**Supplementary Table 1** and **Supplementary Fig. 2** online).

The amino acid substitutions present in CyPet and YPet (**Table 1**) were distributed throughout their structures, with beneficial mutations occurring both proximal and distal to the chromophore (**Supplementary Fig. 3** online). The YPet substitutions H231E and D234N occur in unstructured regions of the X-ray crystal structure[11]. Amino acid substitutions V224L and S208F in YPet conferred RRC enhancement, though neither was fully responsible for the full RRC improvement (data not shown). Additionally, the F46L substitution present in YFP3 has been shown previously to influence the maturation rate of YFP[10]. The chromophore proximal substitution I167A in CyPet was common to three independent CFP variants isolated, possessing similarly altered spectra, and thus is likely responsible for the beneficially altered line shape. Finally, during all rounds of library construction and screening only one substitution was observed within the peptide linker between the FRET pairs, and it did not confer improved FRET (data not shown).

To quantify the benefit of enhanced dynamic range and sensitivity exhibited by the optimized CFP-YFP pair *in vivo*, we compared the ability to detect apoptosis in human embryonic kidney cells (293T) using both the wild-type and the optimized FRET pairs in a caspase-3 substrate (**Fig. 2a–f**). Cells transfected with wild-type CFP-YFP FRET pairs exhibited a range of cyan and yellow fluorescence intensities overlapping with the autofluorescence of nontransfected cells (**Fig. 2a,b**), and a small dynamic range between caspase-3–dependent apoptotic and nonapoptotic cells (**Fig. 2e**). In contrast, cells transfected with the CyPet-YPet substrate expression vector exhibited an improved brightness and dynamic range compared with wild-type CFP-YFP when analyzed by flow cytometry (**Fig. 2c,f**). Owing to improved brightness in both FRET-on and FRET-off states, a larger fraction of the cell population transfected with CyPet-YPet could be resolved from nontransfected cells in both states, despite similar transfection efficiencies (**Fig. 2e,f**). The CyPet-YPet pair therefore makes it possible to identify cells that have initiated caspase-3–dependent apoptosis, and enables high-throughput screening of apoptotic cells using FACS. Thus, application of CyPet-YPet provided both increased signal intensity and enhanced dynamic range between the apoptotic and nonapoptotic populations.

Although FRET could potentially be enhanced through an increased propensity for heterodimerization[9], three observations indicate that this mechanism is unlikely to contribute substantially to FRET improvements. First, analysis by native PAGE confirmed that the evolved fluorescent proteins did not multimerize (**Supplementary Fig. 4** online). Second, concentration-dependent increases in FRET observed in equimolar mixtures of CyPet/YPet were essentially indistinguishable from those observed for the parental pair over the physiologically relevant concentration range of 0.1–100 μM (**Supplementary Fig. 5** online). Finally, cells in the FRET-off state (**Fig. 2f**) exhibited constant YPet:CyPet fluorescence signal ratios with increasing total intracellular concentration. Collectively, these results indicated that dimerization did not occur appreciably under typical assay conditions.

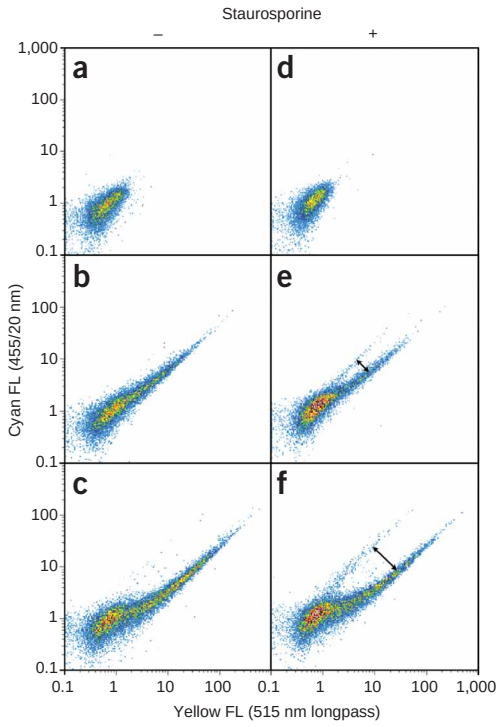

Figure 2 Flow cytometric detection of apoptotic cells using FRET. (**a–f**) Heterogeneous populations of human embryonic kidney (293T) cells were analyzed by flow cytometry before (**a–c**) and after (**d–f**) treatment with the apoptosis inducer staurosporine. Cells were analyzed after mock transfection (**a,d**), after transfection with expression vectors encoding FRET substrates constructed using wild-type CFP-YFP (**b,e**) or CyPet-YPet (**c,f**). Cells undergoing caspase-3-dependant apoptosis (**e,f**) exhibited substantially decreased FRET resulting from substrate cleavage (arrow), enabling high-throughput screening of nonapoptotic and apoptotic cells.

In this study, quantitative, high-throughput FACS was applied to the screening of large fluorescent protein libraries expressed in bacteria for subtle FRET improvements, enabling multistep evolution of the CFP-YFP pair for intracellular FRET. Application of appropriate evolutionary selection pressure is known to be important for enhancement of one or more protein properties, without sacrificing properties not accounted for during screening[12]. The screening of tandem CFP-YFP fusions directly for enhanced FRET signal changes in living cells and cell lysates resulted in improved biochemical and photophysical properties that may not have been obtained using conventional approaches. For example, both CyPet and YPet exhibited improvements in pH sensitivity, which may have been influenced by low intracellular pH resulting from the expression conditions used to achieve optimal FRET. Interestingly, CyPet's emission spectrum exhibited a decreased secondary shoulder, which is expected to enhance FRET detection. Furthermore, the increased line-width enables improved resolution between CyPet and YPet fluorescence signals using standard bandpass filters, without substantially reducing the spectral overlap integral. CyPet's altered line shape was also beneficial for apoptosis detection (**Fig. 2**), wherein cells exhibiting CyPet-YPet cleavage showed subtle but increases in CFP signal intensity relative to that of CFP4-YPet (data not shown).

The optimization of fluorescent proteins for intracellular FRET applications using conventional protein engineering and evolution methodologies has proven challenging[9,13]. Typically, such efforts have focused upon improving the properties of the donor and acceptor independently[5,9,10,13]. Interestingly, the Cerulean variant of the enhanced cyan fluorescent protein (S72A, Y145A, H148D) possesses a 1.55-fold improved quantum yield (QY = 0.62) providing enhanced brightness without a corresponding improvement in the RRC[5]. These results indicate that the dynamic range of fluorescent protein FRET does not correlate well with FRET efficiency predicted by Förster theory. The influence of photophysical properties upon FRET is not straightforward, given the approximation of fluorescent protein chromophores as point-dipoles using Förster's equation[14], the lack of a means to accurately measure the orientation factor and the potentially nonbulk refractive index between the donor and acceptor. Even if these parameters could be measured accurately, the effects of expression, folding, solubility and maturation efficiency strongly influence the measurement of FRET and are difficult to deconvolve from one another.

FACS is unique among protein library screening technologies in that it provides high-throughput screening of single cells at 100,000 per second while enabling the discrimination of subtle changes in cellular fluorescence intensity[15]. Whereas plate-based screening methods have proven useful for routine screening for fluorescent protein improvements, they have not enabled screening for FRET. The ability to quantitatively interrogate 10^8 variants per hour using FACS in this study enabled the screening of large fluorescent protein libraries not accessible to plate-based methods. FACS also provides increased clonal fluorescence resolution capabilities. Cell populations analyzed by FACS that exhibit fluorescence intensity histograms with mean signals differing by twofold overlap substantially owing to the large coefficient of variation associated with a cell population[16]. However, cells exhibiting only twofold improvements can be enriched by sorting the leading edge of the population, regrowing the cells and repeating the process several times[16]. This screening strategy has also been applied for antibody affinity maturation using bacterial and yeast display technologies, allowing isolation of clones with subtly improved binding affinity[16]. In this report, application of multistep screening enabled gradual enrichment of bacterial cells expressing enhanced FRET pairs differing by as little as 1.5-fold between each successive round of evolution. Subtle multiplicative improvements in each round of evolution resulted in a more than sixfold improvement overall, providing enhanced FRET dynamic range (20-fold).

Fluorescent protein FRET pairs have been applied extensively to identify cells undergoing apoptosis by monitoring the proteolytic activity of caspase-3 (refs. 4,17). Such caspase-3 assays have proven useful to screen small libraries of chemical compounds for cellular toxicity in 96-well-plate–based assays[18], as well as to address fundamental questions about the apoptotic pathway[18]. These assays typically possess low sensitivity and throughput precluding their application in high-throughput screening of cells undergoing apoptosis using, for example, flow cytometry. The coupling of flow cytometry with fluorescent protein FRET is especially attractive since photobleaching does not occur appreciably on the time-scale of analysis[19]. Flow cytometric detection of caspase-3 activity in living cells has been accomplished using blue fluorescent protein (BFP)-green fluorescent protein (GFP) FRET[17]. However, since BFP is only weakly fluorescent, rare apoptotic cells (FRET-off state) could not be distinguished from background autofluorescence. In contrast, intracellular expression of the CyPet-YPet caspase-3 substrate enabled improved discrimination of caspase-3 activity, allowing for simple quantification and screening of rare apoptotic cells. The increased dynamic range of CyPet-YPet enables detection and screening of even weak proteolytic activities wherein only a fraction of the substrate is cleaved. In contrast, the small dynamic range of the CFP-YFP pair requires that the majority of substrate in the cell be cleaved to alter the FRET ratio signal. More generally, since CyPet-YPet is efficiently excited by common violet light sources, for example violet diode lasers (405–415 nm), flow cytometric screening on the basis of FRET signals is substantially simplified[19].

Synthetic DNA shuffling has been shown to offer advantages in library construction relative to conventional shuffling of nuclease-generated fragments[20], since it enables efficient recombination and targeted mutagenesis with user-specified amino acid subsets[21]. Synthetic shuffling enabled saturation mutagenesis at positions that strongly influence function from the previous cycle of mutagenesis. For instance, V224I in YFP2 resulted in a roughly 1.5-fold improvement in FRET, but when this position was subjected to synthetic shuffling all isolated mutants possessed V224L (data not shown). Neither mutation has been reported previously. In the YFP crystal structure, V224 is oriented inward toward Y203, which pi-stacks with the chromophore, resulting in red-shifted emission[1]. Thus, it is possible that larger amino acids (isoleucine and leucine) may induce 'second-shell' effects that influence the position of Y203 relative to the chromophore.

The CyPet-YPet pair enables intracellular FRET measurements with enhanced sensitivity and dynamic range, and thus provides the opportunity to perform measurements not tractable with previous pairs. The evolutionary strategy described here could also be applied to a pair consisting of a green donor and a monomeric orange or red fluorescent protein acceptor[9]. However, demand for blue excitable FRET pairs has decreased since violet excitation sources appropriate for CFP have become commonplace in microscopy and flow cytometry instrumentation[22]. CyPet-YPet enables utilization of standard flow cytometry instrumentation for high-throughput analysis and screening applications in signal transduction, protein interactions and enzyme engineering[19]. The ability to perform a wider variety of noninvasive FRET measurements in living cells should be particularly useful in proteomics, metabolic and cellular engineering, and drug discovery.

METHODS

Construction of FRET substrate plasmid. The parental ECFP-YFP caspase substrate was constructed by gene assembly[23]. Oligonucleotides for the assembly of the ECFP (F64L, S65T, Y66W, N146I, M153T, V163A) variant included 5′ flanking *Sac*I and *Sfi*I restriction sites and replacement of the stop codon with a linker region encoding GGSGS and a *Kpn*I restriction site. Genes encoding a caspase-3 cleavage site (DEVD) and YFP (S65G, S72A, K79R, T203Y)[1] were amplified together using gene assembly. The 5′ end of the YFP gene included a *Kpn*I restriction site, bases encoding the caspase-3 site, an *Avr*II restriction site and a GSGGS-encoding linker. *Sfi*I and *Sph*I restriction sites were added at the 3′-end of the YFP gene. The ECFP and linker-YFP gene products were cut and ligated together at the *Kpn*I sites and inserted between the *Sac*I and *Sph*I sites of pBAD33 (ref. 24), resulting in the pB33CCY plasmid. YFP (S65G, S72A, K79R, T203Y) was used as a starting point for directed evolution, since it possessed a higher extinction coefficient (94.54×10^3 M^{-1} cm^{-1}) than other YFPs known upon the initiation of this work.

All cloning and expression experiments were performed using *E. coli* MC1061. Cells were grown overnight at 37 °C in Luria-Bertani (LB) medium supplemented with 0.2% D-(+)-glucose and chloramphenicol. Cultures were diluted 1:100 into LB medium containing chloramphenicol, grown for 2 h at 37 °C, and substrate expression was induced with 0.2% L-(+)-arabinose at 25 °C.

Construction and screening of FRET pair libraries. The first CFP-YFP fusion library was created using error-prone PCR mutagenesis[25] of YFP (S65G, S72A, K79R, T203Y). The YFP PCR product was inserted into pB33CCY as described[26]. The resulting library of 4×10^6 independent transformants possessed a mean error-rate of four mutations per gene. Protein expression was induced for 7 h before each round of sorting. Two rounds of FACS, using a PAS-III flow cytometer (Partec), were used to isolate clones with improved YFP fluorescence. An argon laser (100 mW, 488 nm) was used for excitation and YFP fluorescence was measured at 585 ± 25 nm. In each round, the brightest cells (top 1%) were collected. Before the last round of sorting, induced cultures were incubated at 4 °C for 24 h. The final round of FACS was performed on a FACSAria (BD Biosciences) with 407-nm violet diode laser excitation. The fluorescence of each clone was measured through a 530/30-nm bandpass filter and the brightest cells (top 1%) were sorted into individual wells of a 96-well plate. Fluorimetry with a Cary Eclipse fluorescence spectrophotometer (Varian) was used to scan individual clones for emission between 460 and 560 nm with 433-nm excitation. Clones with an improved 527 to 475 nm emission ratio were collected and further analyzed for RRC improvements *in vitro*.

A second library was constructed targeting both ECFP and YFP for mutagenesis. Mutants of ECFP were generated with error-prone PCR mutagenesis[25] with an average of ten mutations per gene. Synthetic shuffling of improved YFP variants from library 1 using gene assembly mutagenesis[21] resulted in potential diversity of at least 18,432 YFP variants in library 2. Degenerate codons used in YFP mutagenesis were NTC for F46 and I47, VAS for D180 and H231, and NNS for V224, where N = A/C/G/T, V = A/C/G and S = C/G. The CFP-YFP library 2 insert was created by overlap PCR, and ligated into pBAD33 resulting in 5×10^6 independent transformants. Three rounds of FACS with increasingly stringent sort gates were used to enrich clones from library 2 exhibiting increased YFP:CFP emission ratios. A violet diode laser (414 nm) was used for excitation, and CFP and YFP emissions were detected at 455/20 nm and 535/45 nm, respectively. Analysis of 264 clones from the last round of sorting was performed in 96-well plates, and *in vitro* RRC measurements were used to identify improved FRET partners using a Safire fluorescence spectrophotometer (Tecan).

Library 3, an error-prone PCR CFP library, consisted of 1.3×10^7 clones and exhibited an average of four mutations per gene from the parental clone CFP2. Two rounds of FACS were used to isolate bright cyan (455/20 nm emission) clones with 414-nm excitation. The small number of independent CFP clones remaining after these two sorts were transferred to a FRET construct in which each CFP clone was fused to YPet through the caspase-3 linker. This library was sorted once to isolate clones exhibiting strong yellow fluorescence (515-nm longpass) with violet (414 nm) excitation. Individual clones were identified by fluorimetry as described above.

The final library construction, library 4, involved synthetic shuffling of the improved CFP clones found in library 3. The degenerate codons used were RNC for T9, NTC for V11, VAS for D19, VRC for H139, and NNC for I167, E172, L194 and L221, where R=A/G. The total library size from gene assembly mutagenesis was 1.3×10^8 CFP clones. As in library 3, these clones were sorted for high cyan fluorescence then transferred to the FRET construct with YPet and sorted for high yellow fluorescence with violet excitation. The isolated variants were analyzed by fluorimetry to determine the RRC.

***In vitro* measurement of FRET.** For clonal analysis, expression was induced as described above, and approximately 1×10^9 cells were centrifuged at 5,000 r.p.m. for 5 min. Lysates were prepared by using the B-Per II Bacterial Protein Extraction Reagent (Pierce). For FRET-on analysis, 10 µl of lysate was diluted with 190 µl of PBS (pH 7.4). *In vitro* cleavage for FRET-off analysis was achieved by mixing 10 µl of lysate, 30 µl of 50 µg/ml trypsin-EDTA (Invitrogen Life Technologies) and 160 µl PBS (pH 7.4) and incubating for 2 h. The emission intensities of the FRET-on and FRET-off states at 475 nm and 527 nm were determined using fluorimetry with 414-nm excitation and 5-nm emission slits. The FRET ratio change was calculated using: $RRC = (I_{ON}{}^{A} \times I_{OFF}{}^{D})/(I_{ON}{}^{D} \times I_{OFF}{}^{A})$, where $I_y{}^{x}$ is the fluorescence intensity in the y state at the wavelength of maximum emission of x, D is the donor molecule, A is the acceptor molecule, *ON* is the FRET-on state and *OFF* is the FRET-off state. The background fluorescence of lysate obtained from nonfluorescent bacteria was subtracted from all signals before determination of the RRC or relative intensity. The relative emission intensity (with 414-nm excitation) of the lysates (**Fig. 1b**) were measured at 475 nm (the CFP emission maximum) for the FRET-off state and 527 nm (the YFP emission maximum) for the FRET-on state. All FRET-on intensity values were normalized by the CFP-YFP FRET-on intensity and all FRET-off intensity values were normalized by the CFP-YFP FRET-off intensity (**Fig. 1c**). The spectra (**Fig. 1d,e**) were obtained as described above, with the exception that the intensities were divided by the CyPet-YPet RET-on maximum intensity (at 527 nm) for normalization.

Fluorescent protein purification and characterization. C-terminal 6-His–tagged CFPs and YFPs were purified by affinity chromatography using Ni-NTA resin (Qiagen). Protein products were dialyzed against 10 mM Tris, 10 mM EDTA, pH 8.0 for 2 h at 25 °C, 2 h at 4 °C and overnight at 4 °C. The concentration of purified fluorescent proteins was measured using the BCA Assay Kit (Pierce). All spectrophotometric characterizations of the purified proteins were performed at least two weeks after purification using a Safire fluorescence spectrophotometer and corrected by correlation with the known spectrum of 1 mM quinine sulfate in 0.1 N sulfuric acid[14]. Each fluorescent protein was diluted to four different concentrations and the absorbance was measured at the excitation maximum (433 nm for the CFPs and 514 nm for the YFPs). Beer's law was used to determine the extinction coefficient from the slope of a concentration versus absorbance plot. To determine the quantum yield, the absorbance of each purified protein sample was measured at 415 nm for the CFPs and 465 nm for the YFPs. Dilutions between 0.01 and 0.1 absorbance units were made and the corrected emission spectrum of each sample was integrated. Quantum yields were determined by comparison of each integrated spectrum to fluorescein in 0.1 N NaOH (quantum yield of 0.95; ref. 14). The pK_a of the fluorescent proteins were determined as described[5]. Measurements of k_{fold} and k_{ox} were performed as described[27]. These k_{fold} and k_{ox} initial rate values were determined from the first 30 s of fluorescence data.

Mammalian cell expression and analysis. The genes encoding the CFP-YFP, CFP4-YPet and CyPet-YPet caspase-3 substrates were amplified by PCR with the following primers: 5′-GATGGAGTCAAGCTTGAGCTCGGCCACGAAGG CCAGGAG-3′ (forward) and 5′-ATCTGGCGTATCGATGCATGCGGCCACC TTGGCCTTATT-3′ (reverse). The PCR products and the plasmid pLNCX[28] were digested with *Cla*I and *Hin*dIII and ligated. Plasmid DNA was prepared (Qiagen) and 293T cells were transfected as described[29] and grown in DMEM supplemented with 10% FBS. The medium was replaced 1 d after transfection and again 3 d after transfection. The cells were trypsinized 4 d after transfection and half of the cells were exposed to 1 µM staurosporine (Sigma), an apoptosis inducer, for 6 h. The cells were spun down at 2,500 r.p.m. for 4 min and resuspended in PBS (pH 7.4). Transfection efficiency was approximately 50–60%, as determined by flow cytometry (488-nm excitation). Cytometric analysis of FRET was performed using violet diode laser excitation (414 nm), a

455/20-nm bandpass filter for cyan detection, and a 515-nm longpass filter for yellow detection.

Note: Supplementary information is available on the Nature Biotechnology website.

ACKNOWLEDGMENTS

We wish to acknowledge E. Lipman for helpful discussions, A. Mikhailovsky and D. Korystov for lifetime measurement assistance and P. Bessette for critically reading the manuscript. We further acknowledge the generous support of this project by the National Institutes of Health-National Institute of Biomedical Imaging and Bioengineering grant EB-000205 and a National Science Foundation graduate fellowship to A.W.N.

COMPETING INTERESTS STATEMENT

The authors declare that they have no competing financial interests.

Received 26 August; accepted 6 December 2004
Published online at http://www.nature.com/naturebiotechnology/

1. Tsien, R.Y. The green fluorescent protein. *Annu. Rev. Biochem.* **67**, 509–544 (1998).
2. Miyawaki, A. *et al.* Fluorescent indicators for Ca^{2+} based on green fluorescent proteins and calmodulin. *Nature* **388**, 882–887 (1997).
3. Chan, F.K. *et al.* Fluorescence resonance energy transfer analysis of cell surface receptor interactions and signaling using spectral variants of the green fluorescent protein. *Cytometry* **44**, 361–368 (2001).
4. Jones, J., Heim, R., Hare, E., Stack, J. & Pollok, B.A. Development and application of a GFP-FRET intracellular caspase assay for drug screening. *J. Biomol. Screen.* **5**, 307–318 (2000).
5. Rizzo, M.A., Springer, G.H., Granada, B. & Piston, D.W. An improved cyan fluorescent protein variant useful for FRET. *Nat. Biotechnol.* **22**, 445–449 (2004).
6. Jensen, K.K., Martini, L. & Schwartz, T.W. Enhanced fluorescence resonance energy transfer between spectral variants of green fluorescent protein through zinc-site engineering. *Biochemistry* **40**, 938–945 (2001).
7. Van Der Meer, B.W., Coker, G. & Chen, S.Y.S. *Resonance Energy Transfer Theory and Data* (VCH Publishers, New York, 1994).
8. Pollok, B.A. & Heim, R. Using GFP in FRET-based applications. *Trends Cell Biol.* **9**, 57–60 (1999).
9. Campbell, R.E. *et al.* A monomeric red fluorescent protein. *Proc. Natl. Acad. Sci. USA* **99**, 7877–7882 (2002).
10. Nagai, T. *et al.* A variant of yellow fluorescent protein with fast and efficient maturation for cell-biological applications. *Nat. Biotechnol.* **20**, 87–90 (2002).
11. Rekas, A., Alattia, J.R., Nagai, T., Miyawaki, A. & Ikura, M. Crystal structure of venus, a yellow fluorescent protein with improved maturation and reduced environmental sensitivity. *J. Biol. Chem.* **277**, 50573–50578 (2002).
12. Voigt, C.A., Kauffman, S. & Wang, Z.G. Rational evolutionary design: the theory of *in vitro* protein evolution. *Adv. Protein Chem.* **55**, 79–160 (2000).
13. Heim, R. & Tsien, R.Y. Engineering green fluorescent protein for improved brightness, longer wavelengths and fluorescence resonance energy transfer. *Curr. Biol.* **6**, 178–182 (1996).
14. Lakowicz, J.R. *Principles of fluorescence spectroscopy*, edn. 2 (Kluwer Academic/Plenum Publishers, New York, 1999).
15. Georgiou, G. Analysis of large libraries of protein mutants using flow cytometry. *Adv. Protein Chem.* **55**, 293–315 (2000).
16. Boder, E.T. & Wittrup, K.D. Optimal screening of surface-displayed polypeptide libraries. *Biotechnol. Progr.* **14**, 55–62 (1998).
17. Xu, X. *et al.* Detection of programmed cell death using fluorescence energy transfer. *Nucleic Acids Res.* **26**, 2034–2035 (1998).
18. Takemoto, K., Nagai, T., Miyawaki, A. & Miura, M. Spatio-temporal activation of caspase revealed by indicator that is insensitive to environmental effects. *J. Cell Biol.* **160**, 235–243 (2003).
19. He, L. *et al.* Flow cytometric measurement of fluorescence (Forster) resonance energy transfer from cyan fluorescent protein to yellow fluorescent protein using single-laser excitation at 458 nm. *Cytometry* **53**, 39–54 (2003).
20. Ness, J.E. *et al.* Synthetic shuffling expands functional protein diversity by allowing amino acids to recombine independently. *Nat. Biotechnol.* **20**, 1251–1255 (2002).
21. Bessette, P.H., Mena, M.A., Nguyen, A.W. & Daugherty, P.S. Construction of designed protein libraries using gene assembly mutagenesis. in *Directed Evolution Library Creation Methods and Protocols,* vol. 231 (eds. Arnold, F.H. & Georgiou, G.) 29–37, (Humana Press, Totowa, 2003).
22. Shapiro, H.M. & Perlmutter, N.G. Violet laser diodes as light sources for cytometry. *Cytometry* **44**, 133–136 (2001).
23. Stemmer, W.P., Crameri, A., Ha, K.D., Brennan, T.M. & Heyneker, H.L. Single-step assembly of a gene and entire plasmid from large numbers of oligodeoxyribonucleotides. *Gene* **164**, 49–53 (1995).
24. Guzman, L.M., Belin, D., Carson, M.J. & Beckwith, J. Tight regulation, modulation, and high-level expression by vectors containing the arabinose PBAD promoter. *J. Bacteriol.* **177**, 4121–4130 (1995).
25. Fromant, M., Blanquet, S. & Plateau, P. Direct random mutagenesis of gene-sized DNA fragments using polymerase chain reaction. *Anal. Biochem.* **224**, 347–353 (1995).
26. Miyazaki, K. & Takenouchi, M. Creating random mutagenesis libraries using megaprimer PCR of whole plasmid. *Biotechniques* **33**, 1033–1038 (2002).
27. Reid, B.G. & Flynn, G.C. Chromophore formation in green fluorescent protein. *Biochemistry* **36**, 6786–6791 (1997).
28. Miller, A.D., Miller, D.G., Garcia, J.V. & Lynch, C.M. Use of retroviral vectors for gene transfer and expression. *Methods Enzymol.* **217**, 581–599 (1993).
29. Miller, A.D. & Rosman, G.J. Improved retroviral vectors for gene transfer and expression. *Biotechniques* **7**, 980–990 (1989).